Modeling Bias Dependence of Self-Heating in GaN HEMTs Using Two Heat Sources

Xuesong Chen, Slim Boumaiza, Lan Wei

Department of Electrical and Computer Engineering, University of Waterloo

2020/07/01

IEEE TRANSCATIONS ON ELECTRON DEVICES (IF=2.917)

Overview

- Being the result of Joule heating, self-heating is highly bias dependent, *i.e*. dependent on drain voltage and gate voltage.
- Previous thermal studies on self-heating assumed a single heat source located right under the gate, these single heat source approaches can not account for the bias dependence of self-heating. Also, the bias dependence of self-heating in GaN HEMTs has not been studied quantitatively.
- This work proposed two-heat-source model to capture the bias dependence of the heat and temperature distribution in the GaN HEMT channel without resorting to the more resource-intensive electrothermal simulations.

Bias Dependence of Self-Heating

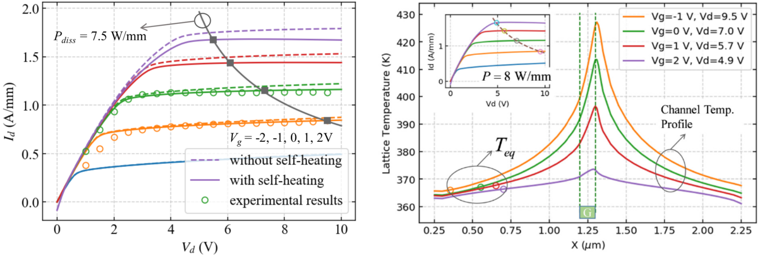

(a) Output characteristics of the HEMT.

(b) Channel temperatures with the same power dissipation $P_{\text{diss}} = 8\,\text{W}/\text{mm}$.

Figure 1: Bias dependence of self-heating in GaN HEMTs.

Schematic of the HEMT

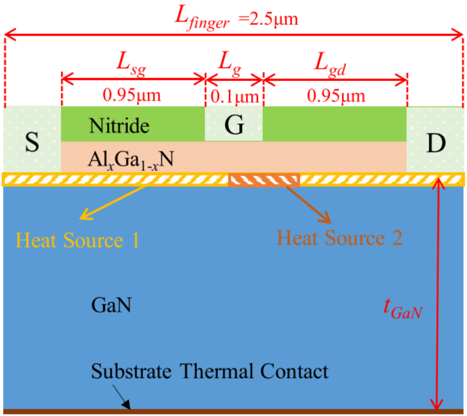

Figure 2: Schematic of the HEMT under study. The geometries are note drawn to scale.

Two Regions in the channel

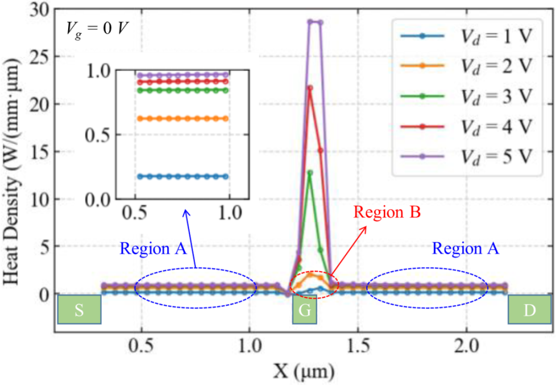

Figure 3: Heat density along the HEMT channel at $V_g = 0$ V and $V_d = 1$ V to 5 V.

Heat Density in Two Regions

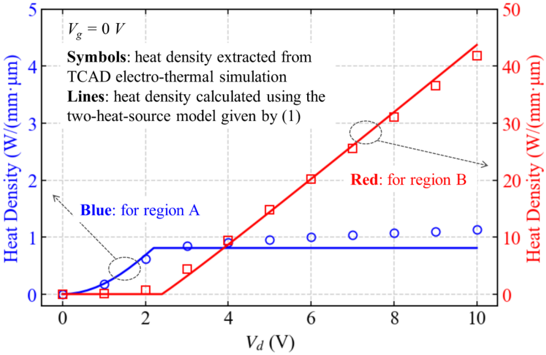

Figure 4: Heat density in region A and region B versus drain voltage V_d.

1. Background
2. Two-Heat-Source Model
    - Bias-Dependent Heat Generation
    - Two-Heat-Source Model
    - Model Validation
3. Maximum Channel Temperature
4. Conclusion
5. Discussions on t_{GaN}
6. Perspective

Two-Heat-Source Model

$$\begin{cases} P_1 = I_\mathrm{d} V_\mathrm{d}, \quad P_2 = 0, & \text{for} \quad V_\mathrm{d} \leq V_\mathrm{dsat} \\ P_1 = I_\mathrm{d} V_\mathrm{dsat}, \quad P_2 = I_\mathrm{d}\left(V_\mathrm{d} - V_\mathrm{dsat}\right), & \text{for} \quad V_\mathrm{d} > V_\mathrm{dsat} \end{cases}$$

- P_1 corresponds to the uniform heat generated in the low-field regions. In the linear regime ($V_d \leq V_\mathrm{dsat}$), all the generated heat is dissipated through HS1.
- P_2 is associated with the small high-field region around the drain-side gate edge when the device is in saturation. In the saturation regime ($V_d > V_\mathrm{dsat}$), the heat dissipated by HS1 is capped to its maximum value, whereas HS2 dissipates the additional heat due to the increased V_d.
- $L_\mathrm{HS1} = L_\mathrm{finger}, L_\mathrm{HS2} = 0.16\,\mu\mathrm{m}$

Heat Dissipation for the Two Heat Sources

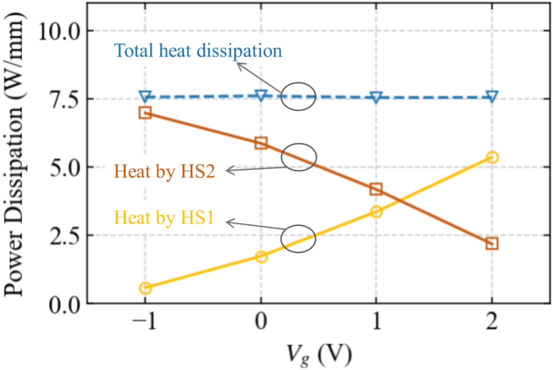

Figure 5: Heat dissipation for the two heat sources predicted by THS model for four different biases that give the same total power dissipation $P_{\text{diss}} = 7.5\,\text{W}/\text{mm}$.

Bias-Dependent Channel Temperature

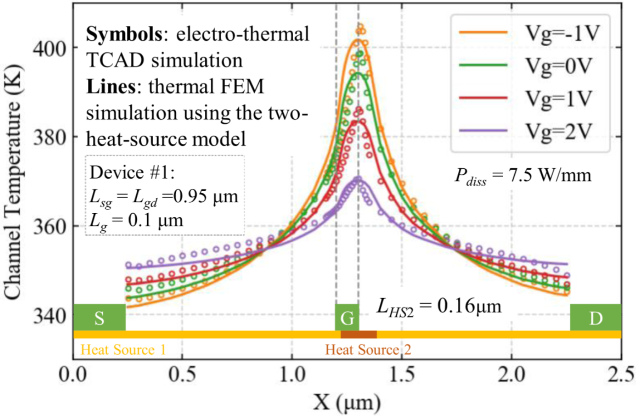

Figure 6: Temperature profiles across the channel at $P_{\text{diss}} = 7.5\,\text{W}/\text{mm}$ and the four different biases. The symbols are acquired from electrothermal TCAD simulations; the lines generated from thermal-only FEM simulation based on THS model.

Bias-Dependent Channel Temperature

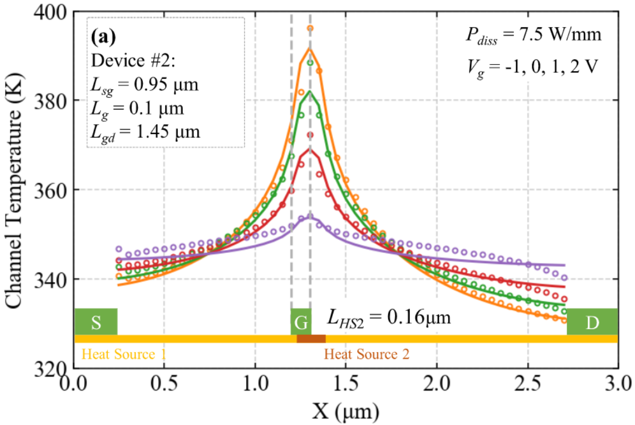

Figure 7: Device 2 with longer drain access region $L_{sg} = 0.95\,\mu m, L_g = 0.1\,\mu m, L_{gd} = 1.45\,\mu m$.

Bias-Dependent Channel Temperature

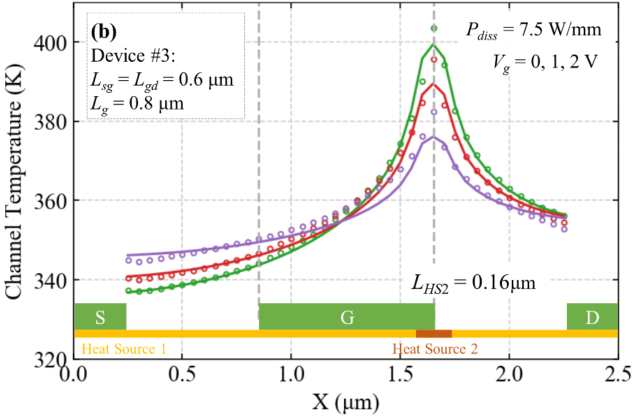

Figure 8: Device 3 with longer gate length $L_{\text{sg}} = 0.6\,\mu\text{m}, L_{\text{g}} = 0.8\,\mu\text{m}, L_{\text{gd}} = 0.6\,\mu\text{m}$.

Thermal Resistance Model

Two-heat-source model

$$\begin{cases} P_1 = I_\mathrm{d} V_\mathrm{d}, \quad P_2 = 0, & \text{for} \quad V_\mathrm{d} \le V_\mathrm{dsat} \\ P_1 = I_\mathrm{d} V_\mathrm{dsat}, \quad P_2 = I_\mathrm{d} \left(V_\mathrm{d} - V_\mathrm{dsat} \right), & \text{for} \quad V_\mathrm{d} > V_\mathrm{dsat} \end{cases}$$

$$T_\mathrm{max} = T_0 + (R_\mathrm{sub} + R_1) P_1 + (R_\mathrm{sub} + R_2) P_2$$

- R_sub denotes Thermal boundary resistance.
- R_1 denotes unidimensional thermal resistance by HS1 in the linear regime.
- R_2 denotes thermal spreading resistance by HS2 in the saturation regime.

Bias-Dependent Maximum Temperature

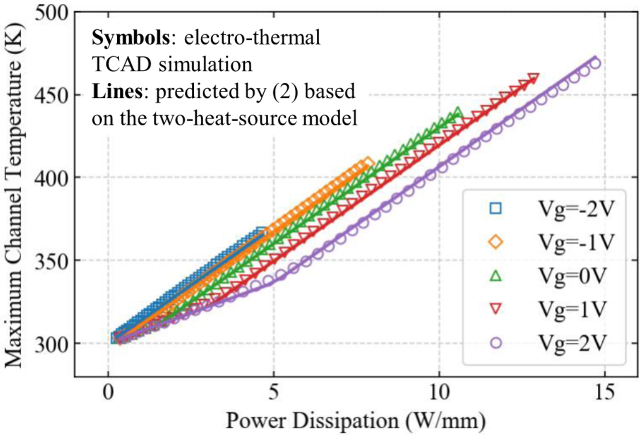

Figure 9: Maximum channel temperature T_{max} versus total power dissipation P_{diss} of the GaN HEMT at different biases extracted from electrothermal TCAD simulations (symbols) and reproduced using the proposed analytical model.

Differential Thermal Resistance

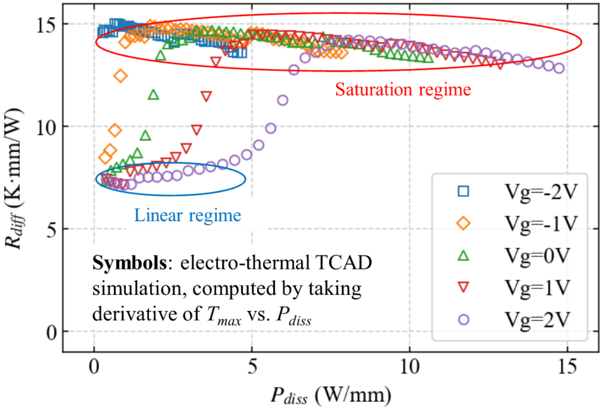

Figure 10: Differential thermal resistance R_{diff}, computed as the derivative of T_{max} versus P_{diss}. The linear-regime value $R_{\text{diff, lin}}$ and saturation-regime value $R_{\text{diff, sat}}$ are extracted to be 7.3 and $14\,\text{K mm}/\text{W}$, respectively.

Thermal Resistance Analysis

Table 1: Themal spreading resistance R_2 from electrothermal simulations for various device geometries (in µm).

L_g	R_2	L_{sg}	R_2	L_{gd}	R_2	t_{GaN}	R_2
0.075	9.9	0.45	11.0	0.45	11.5	0.5	8.5
0.1	10.0	0.95	10.0	0.95	10.0	1.0	10.0
0.8	10.7	1.45	9.4	1.45	9.0	2.0	13.3

Conclusion

- The article presented a new approach to model self-heating in GaN HEMTs using two heat sources.
- The proposed two-heat-source thermal model accurately captures the bias dependence of the self-heating phenomenon in GaN HEMTs.
- The proposed model also leads to a simple and accurate expression for the maximum channel temperature.

Discussions on t_{GaN}

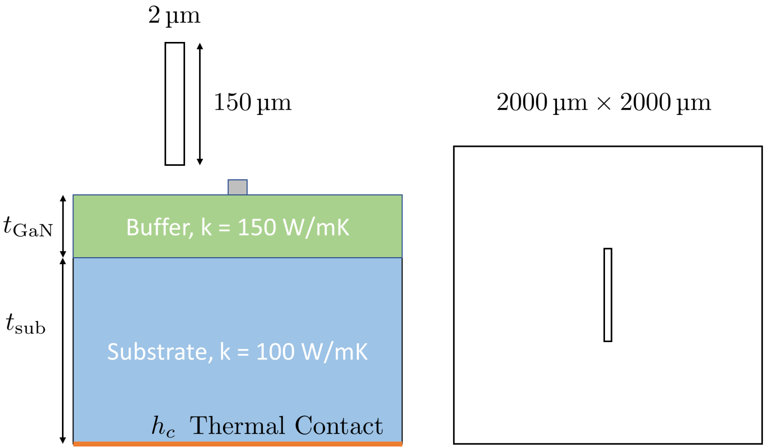

Figure 11: Schematic of the modeled device, $q = 1 \times 10^{10}\ \mathrm{W/m^2}$.

Temperature Feild

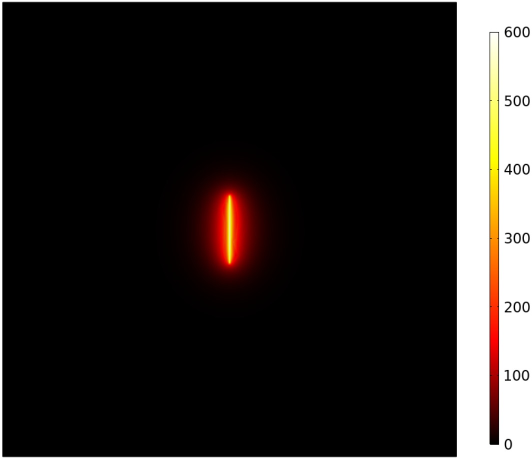

Figure 12: Top view temperature field of the simulated device, $h_c = 0.5 \times 10^8\,\mathrm{W/m^2\,K}$, $t_{\mathrm{GaN}} = 1\,\mu\mathrm{m}$, $t_{\mathrm{sub}} = 100\,\mu\mathrm{m}$.

Effects of h_c on t_{GaN}

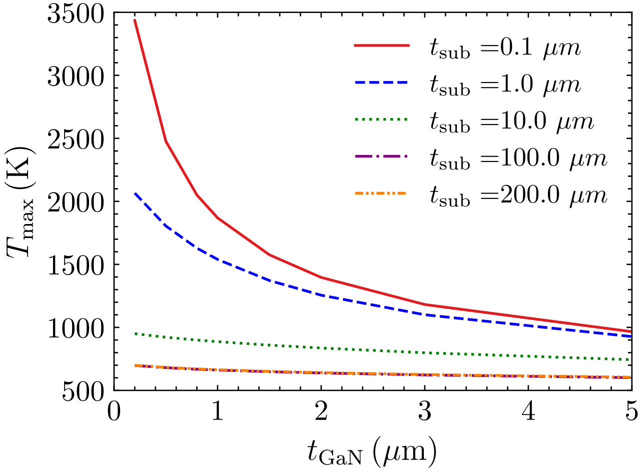

Figure 13: The maximum temperature of the device as a function of t_{GaN}, $h_c = 6.5 \times 10^5\,\mathrm{W/m^2\,K}$.

Effects of h_c on t_{GaN}

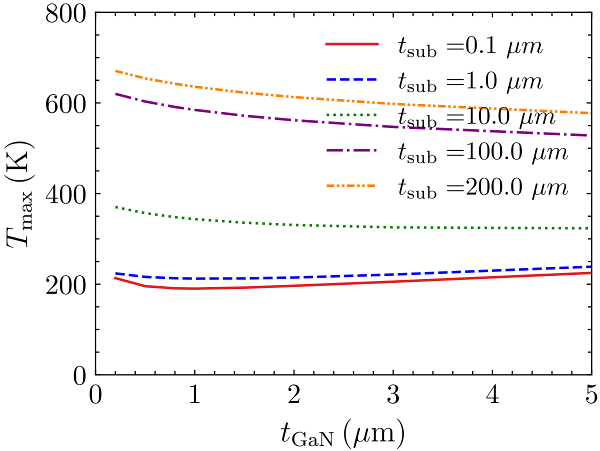

Figure 14: The maximum temperature of the device as a function of t_{GaN}, $h_c = 0.5 \times 10^8\,\mathrm{W/m^2\,K}$.

Effects of h_c on t_{GaN}

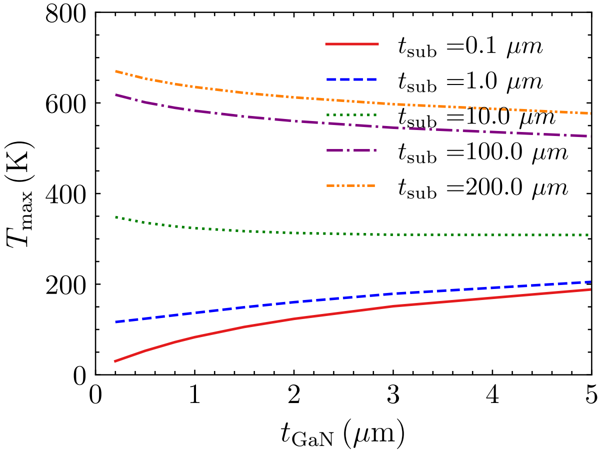

Figure 15: The maximum temperature of the device as a function of t_{GaN}, isothermal thermal contact.

Effects of t_{sub} on $T_{\max}$

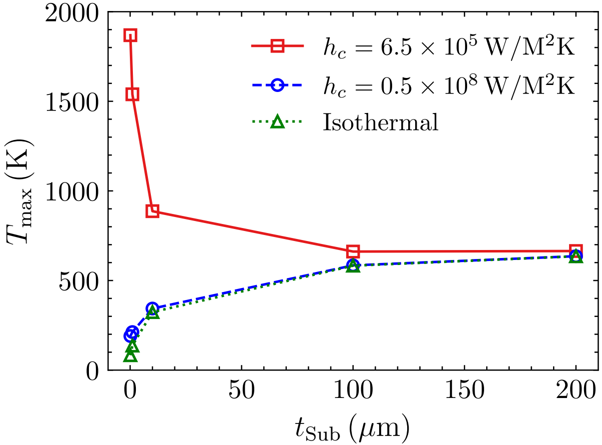

Figure 16: The maximum temperature of the device as a function of t_{sub}, $t_{\text{GaN}} = 1\,\mu\text{m}$.

Effects of t_{sub} on T_{max}

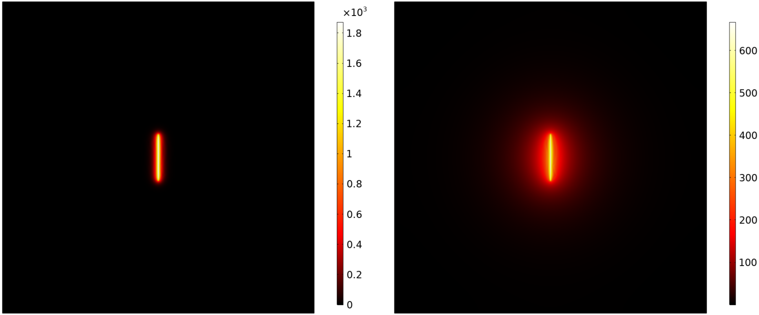

(a) $t_{sub} = 0.1\,\mu\text{m}$ (b) $t_{sub} = 100\,\mu\text{m}$

Figure 17: Top view temperature field of the simulated device, $t_{\text{GaN}} = 1\,\mu\text{m}$, $h_c = 6.5 \times 10^5\,\text{W}/\text{m}^2\,\text{K}$.

Some Insights

When $k_{\text{buffer}} > k_{\text{substrate}}$:

- When h_c is low and t_{sub} is not too low, increasing t_{GaN} will enhance thermal spreading in GaN layer and reduce the juncture temperature (real situation).
- When h_c is high (limit to isothermal condition) and t_{sub} is low, decreasing t_{GaN} will lead the heat in GaN layer directly flow to the heat sink and reduce the juncture temperature (unreal).
- When h_c is low, properly increasing t_{sub} will enhance thermal spreading in the device and reduce the juncture temperature (non consider envelope).
- The above conclusions only consider two layers and don't include the influences of ballistic effects.

Thermal Resistance with Bias Dependence and Phonon Transport

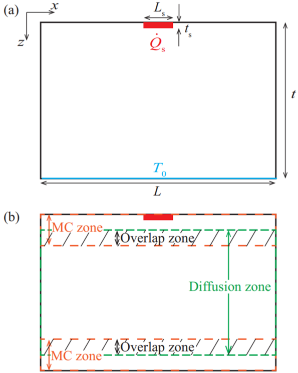

+

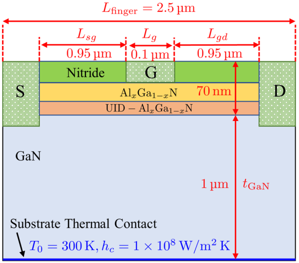

$$\frac{R}{R_{1\text{–D\_}0}} = \frac{R_F}{R_{1\text{–D\_}0}}\left(1 + \frac{2}{3}Kn_t\right)(1 + A_w Kn_w)$$

Finished Work

TCAD+FEM Simulation Process

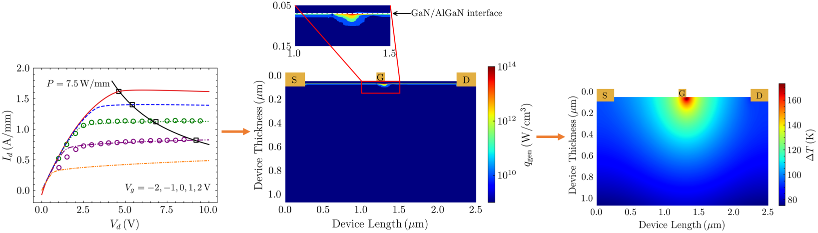

Perspective Roadmap

Gray Model

$$R_F\left(1+\frac{2}{3}Kn_t\right)(1+A_wKn_w)$$

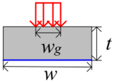

Gray MC

Various Factors

Dispersion

Heat Source

Bias Dependence

Interfaces

Multi-finger

……

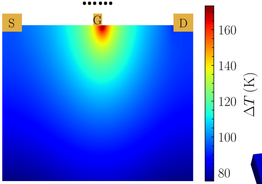

Various Techniques

Dispersion MC

TCAD Simulations

Electron-Phonon MC

……

Effective Thermal Conductivity

+

FEM

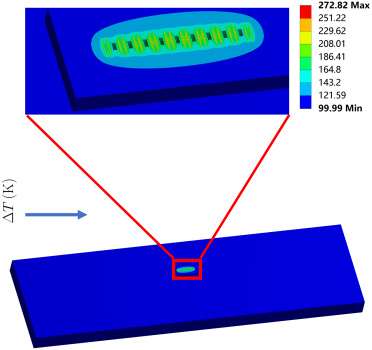

Multiscale Electrothermal Simulations

Thank You!